

## Inflation rate of the Colli Albani volcanic complex retrieved by the permanent scatterers SAR interferometry technique

S. Salvi,<sup>1</sup> S. Atzori,<sup>1</sup> C. Tolomei,<sup>1</sup> J. Allievi,<sup>2</sup> A. Ferretti,<sup>3</sup> F. Rocca,<sup>3</sup> C. Prati,<sup>3</sup> S. Stramondo,<sup>1</sup> and N. Feuillet<sup>1</sup>

Received 14 April 2004; accepted 20 May 2004; published 22 June 2004.

[1] We analyzed 99 ERS SAR images of the Colli Albani volcano using the Permanent Scatterers technique. We retrieved the average surface displacement velocities for over 100,000 scatterers for the period 1993–2000, showing that present deformation is concentrated in the area of most recent volcanic activity, with rates up to 2.6 mm/yr in the satellite line of sight. We inverted the observed deformation using several analytical solutions for volcanic sources in an elastic half space. The best fit is obtained with two Mogi sources aligned in a N-S direction at 5 and 7 km depth beneath the western flank of the volcano. *INDEX TERMS*: 1243 Geodesy and Gravity: Space geodetic surveys; 8145 Tectonophysics: Physics of magma and magma bodies; 8494 Volcanology: Instruments and techniques. *Citation*: Salvi, S., S. Atzori, C. Tolomei, J. Allievi, A. Ferretti, F. Rocca, C. Prati, S. Stramondo, and N. Feuillet (2004), Inflation rate of the Colli Albani volcanic complex retrieved by the permanent scatterers SAR interferometry technique, *Geophys. Res. Lett.*, 31, L12606, doi:10.1029/2004GL020253.

### 1. Introduction

[2] The Colli Albani volcano (Figure 1) is a 0.6 ma-old caldera complex, located 15 km SE of Rome, Italy. It belongs to one of the Upper Pleistocene, alkali-potassic volcanic districts originated on the Tyrrhenian margin of the Italian peninsula, during the post-Messinian extensional tectonic phase [De Rita *et al.*, 1995]. It is considered a quiescent volcano, whose last erupted products have been radiometrically dated at 20 ka [De Rita *et al.*, 1995]. In the area of most recent activity (maar lakes of Albano and Nemi), periodic unrest episodes have been directly observed and documented since the early Roman age [Funciello *et al.*, 2003] manifested as intermittent swarms of shallow, moderate magnitude earthquakes (Figure 1) [e.g., Chiarabba *et al.*, 1997], occasional episodes of magmatic CO<sub>2</sub> release [Pizzino *et al.*, 2002], and pulses of surface uplift [Amato and Chiarabba, 1995]. This activity has been going on since at least early Holocene times, as suggested by the presence of lahar deposits originated during catastrophic lake over-spills [Funciello *et al.*, 2003].

[3] The most recent and important seismic unrest episode occurred in 1989–1990. Between 1951 and 1994 a considerable ground uplift (up to 30 cm) was recorded by levelling

along two lines crossing the maar lakes area [Amato and Chiarabba, 1995]. Volcanic source geometry and volume were estimated by modelling these data [Chiarabba *et al.*, 1997], and Feuillet *et al.* [2004] showed that the swarm was triggered by Coulomb stress changes induced by the volcanic inflation.

[4] To retrieve the deformation field at a higher spatial resolution, we applied the Permanent Scatterers analysis on ERS1-2 descending and ascending SAR images. The new data set clearly shows the inflation patterns of the Colli Albani in the period 1993–2000. We use the data to constrain preliminary analytic models of the source.

### 2. Surface Deformation From Permanent Scatterers Analysis

[5] The PS technique is a recent methodological development of the classical Differential SAR Interferometry, which allows an improvement of the measurement accuracy, providing estimates of ground displacement velocity of mm/years [Ferretti *et al.*, 2001]. In the PS technique, long time series of SAR images are used, and only the natural targets showing a good stability of the backscattered signal in all the images (Permanent Scatterers, hereinafter PS) are considered for the calculation of the phase differences between acquisitions. A specific filtering algorithm is used to estimate and remove the tropospheric contribution from the phase signal, restoring the ground displacement velocity for each PS, in the line of sight of the SAR antenna (slant range). For a complete description of the PS technique refer to Ferretti *et al.* [2001].

[6] The PS technique has been applied to the Colli Albani area using 66 ERS1-2 images relative to descending orbits and 33 images from ascending orbits, acquired in the period 1993–2000. Over 47,000 PS with a coherence greater than 0.70 were identified on the descending images and over 53,000 PS were detected on the ascending images using a coherence threshold of 0.77. Note that generally the PS coincide with buildings or man-made structures, whose density is very high in the urban areas. Although the lack of urban settlements and favorable rock outcrops causes the presence of several “no-data” zones, the general pattern of the velocity field is rather clear, and confirms the presence of a N-S uplift zone around the western border of the caldera, in the area of most recent phreatomagmatic activity, allowing to define the deformation patterns with unprecedented resolution (Figures 2 and 3).

### 3. Data Validation and Analysis

[7] Independent ground data have been used for the validation of the remote sensing observations and for the

<sup>1</sup>Istituto Nazionale di Geofisica e Vulcanologia, Rome, Italy.

<sup>2</sup>TeleRilevamento Europa, Milan, Italy.

<sup>3</sup>Dipartimento di Elettronica e Informazione, Politecnico di Milano, Milan, Italy.

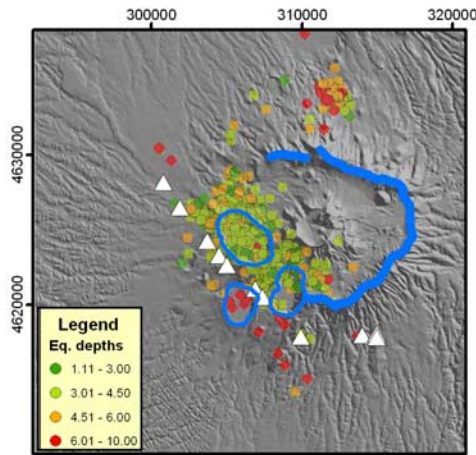


**Figure 1.** Shaded relief of the Colli Albani volcano showing earthquake locations for the 1989–1990 seismic unrest period. Also shown are the leveling benchmarks for the IGMI line (see text) and the location of the INGR CGPS station used as reference for the PS velocity maps.

establishment of a common reference point for the ascending and descending velocity maps. We first compared the PS slant range ground velocities to the leveling data produced by the Italian Military Geographical Institute – IGMI, using the average vertical velocities (i.e., calculated considering a constant ground displacement rate) resulting from the 1951–1997 height differences. We calculated the average PS ground velocity for each of the 10 leveling benchmarks (Figure 1) considering all PS falling in a circular radius of 200 m. As shown in Figure 4, the curves display a similar general trend, the main discrepancies being a quasi-symmetric shift of the PS-data ascending and descending maxima with respect to the leveling one, and a factor of  $\sim 3$  difference in the peak velocity values (although note that there is no difference at the borders of the deformation zone). The curve shift indicates the presence of a horizontal component of ground displacement, which translates to different slant range displacements when projected in the ascending and descending orbit geometry. The difference in velocity values

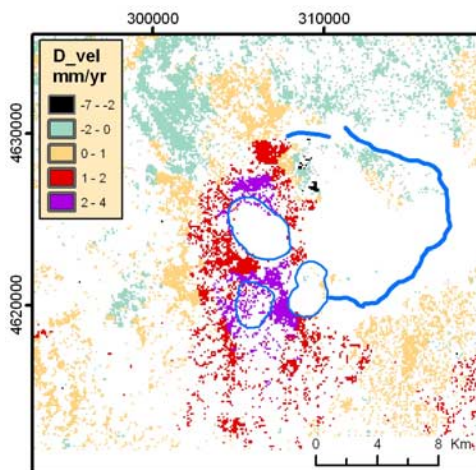


**Figure 2.** Ground velocity in the period 1993–2000, in the Line of Sight of the descending ERS orbit. The site of the Solfiorata gas vents is indicated (S).

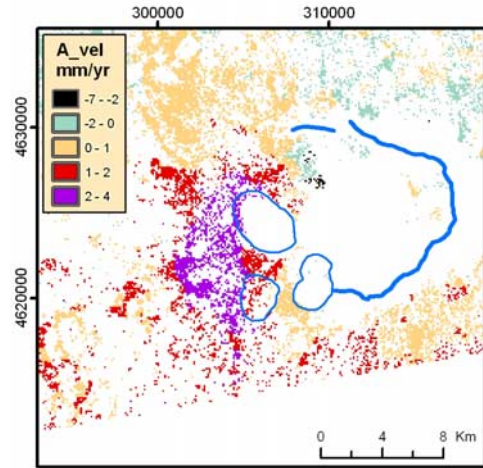


**Figure 3.** Ground velocity in the period 1993–2000, in the ascending ERS orbit. Also shown is the dislocation area for our model 1S. The site of the Solfiorata gas vents is indicated (S).

was also expected, given the different time span of the leveling and PS data sets (47 vs. 8 years) and the strong time dependence of surface deformation processes commonly observed in volcanic areas. In fact our observations indirectly confirms that the uplift rate in the Colli Albani increases in connection with seismic unrest events, as already noted by *Chiarabba et al.* [1997], who suggested that most of the ground deformation in the leveling data occurred during the last important seismic crisis (1989–1990).

[8] A survey-mode GPS network of 10 benchmarks was deployed and measured in the Colli Albani in 1995, 1996, 1997, 1998 [*Anzidei et al.*, 1998]; unfortunately the only three monuments yielding significant velocity estimates fall in areas with no PS. Continuous GPS data from 2000 to 2003 at the INGR station (Figure 1) show the absence of local horizontal velocity components and a negative vertical velocity ( $\sim 1$  mm/y, F. Riguzzi, personal communication, 2004). We used the INGR site, located  $\sim 20$  km from the uplift centre, as reference, rescaling the ascending and descending PS velocities accordingly.

[9] Notwithstanding the scarcity of data in the central-eastern caldera ring due to low multi-temporal coherence, the general deformation pattern is rather clear and shows that the highest velocities are concentrated in the area of the

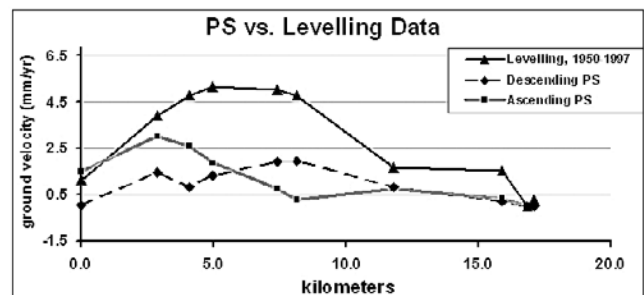


**Figure 4.** Comparison between the ground velocities retrieved by the PS technique in the 1993–2000 period, and the average ground velocity retrieved by leveling in the 1997–1950 period.

**Table 1.** Modeling Parameters and Modeled Injection Volumes for Sources S2 and M2

Model	North, km	East, km	Strike, deg.	Dip, deg.	Length, km	Width, km	Depth, km	$\Delta V$ , km <sup>3</sup> /yr	RMS	$\Delta P^a$
S2 North	4624.2	304.8	16	0	9.0	0.5	5.0	2.0E-04	0.54	
S2 South	4614.4	306.2	225	6	8.5	4.0	9.0	3.4E-04	0.54	
M2 North	4624.8	305.9					4.6	2.0E-04	0.57	1.9E + 06
M2 South	4615.3	304.7					7.2	4.4E-04	0.57	4.2E + 06

<sup>a</sup>For Mogi (1 km-radius) in Pa.

Albano, Ariccia and Nemi craters. Although the general pattern is N-S, the deformation is not symmetrical to a N-S axis, and a slightly eastward concavity is evident (Figures 2 and 3). The ground velocities decrease radially from this alignment down to about 0 in  $\sim 15$  km (for the ascending data) and  $\sim 8$  km (for the descending data); for both data sets the deformation is broader in the southern side of the volcanic edifice and more peaked in the northern side (Figures 2 and 3). This general trend shows only two important deviations; the first one lies NE of the Albano lake, where a limited area ( $1 \times 3$  km) of strong subsidence is present (Figures 2 and 3). Given the general similarity of ascending and descending velocities, with values up to  $-3$  mm/yr, we estimate the ground displacement here to be mainly vertical. We attribute the subsidence to sediment compaction due to the strong water pumping which has caused in several zones of the Colli Albani a considerable lowering of the water table. Another area deviating from the general trend is located SW of the main edifice, towards the Tyrrhenian coast. Here both data sets indicate high positive velocities ( $\sim 1.3$  mm/yr) over an area of  $8 \times 8$  km, suggesting the presence of a deep source. The volcanic origin of the latter is suggested by the coincidence with hydrothermal manifestations (the Solfiorata gas vents), where the isotopic composition of the gases shows a deep origin [Boni *et al.*, 1995]. Long term uplift of this area is also testified by the anomalous high elevations of the base of the volcanic products and by the peculiar modification of the general trend of the drainage network orientation and density [De Rita *et al.*, 1992].

[10] The shift of the ascending and descending maxima visible in Figure 4 is also evident in the velocity maps (Figures 2 and 3) and confirms the symmetry of the horizontal deformation with respect to the midpoint between the two zones. We recall that the angular separation between the ascending and descending tracks on the ground is  $\sim 24^\circ$ , and that the slant range direction is inclined  $\sim 23^\circ$  from the vertical, looking East or West during ascending or descending orbits, respectively. Therefore an eastward displacement of a point on the ground is seen as an ‘uplift’ in the descending Line of Sight (LoS), and a ‘subsidence’ in the ascending LoS, and vice versa.

#### 4. Source Modelling

[11] We used the ascending and descending PS ground velocities to constrain source models for the total inflation observed in the 8-year period. Prior to the modelling, we low pass-filtered the velocity maps using a  $500 \times 500$  m moving window to smooth the high frequency components. We also excluded from the model fit calculations the two areas described in the previous section for which we hypothesised a different source.

[12] We attempted to model the inflation source using three different source mechanisms: the analytical solutions by

Okada [1985] for a rectangular, purely tensile dislocation in a Poissonian elastic half space (sill), the Mogi [1958] solutions for a point-pressure source, and the Yang *et al.* [1988] solutions for a spheroid pressure source. We used a non-linear inversion algorithm based on Simulated Annealing [Sen and Stoffa, 1995]. The cost function to minimise is based on a simultaneous least-squares fit to both ascending and descending PS data sets. The cooling sequence follows the law  $T(i) = k \cdot T_0$  with  $T_0 = 0.999$  and the system is considered cold when the cost function is stable for at least 10 cycles [Atzori, 2004]. Since the average topographic slope in the area is small ( $\sim 8^\circ$ ), with maximum elevation differences of  $\sim 400$  m, in the inversion we neglected the effects of topography on the deformation field, possibly causing a 10% increase of source depth uncertainties [Cayol and Cornet, 1998].

[13] Given the N-S elongation of the velocity field, inverting for a single source results in long and narrow sills or spheroids (we found lengths of 16 and 22 km, respectively, and widths of 1 and 1.5 km), which cannot be reconciled with volcanological and seismological observations [Chiarabba *et al.*, 1997]. Nevertheless, both sources plunge to the south, suggesting that the deformation may result from two sources located at different depths. Our preferred solution has two Mogi sources aligned  $\sim$ N-S separated by a distance of 7 km with a depth of  $\sim 5$  km for the northern one and  $\sim 7$  for the southern one (M2 in Table 1). Residuals for descending and ascending data sets are shown in Figures 5 and 6. We also tested a model with two tensile Okada sources but we did not obtain a significantly improved fit to the observations (S2 in Table 1).

#### 5. Discussion

[14] The M2 sources are located in the area of most recent volcanic activity. Several phreatomagmatic explosions origi-

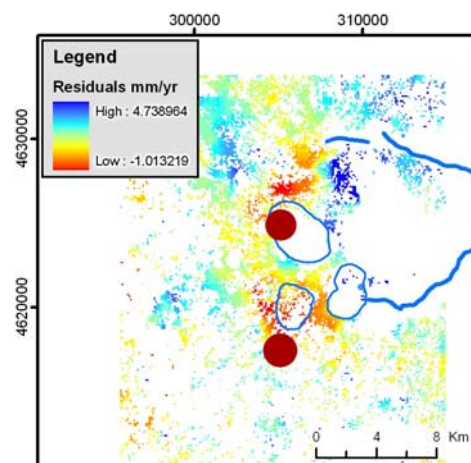


**Figure 5.** Residuals (Model-Observations) for our model M2 in the descending LoS.

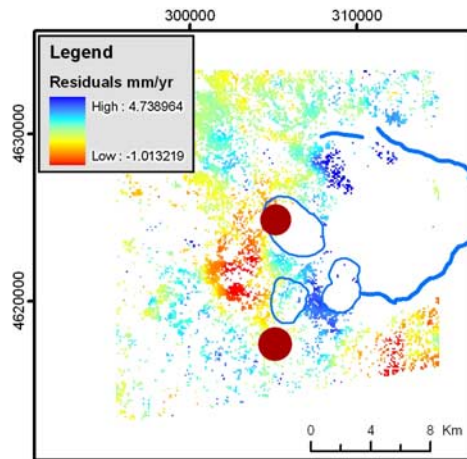


**Figure 6.** Residuals (Model-Observations) for our model M2 in the ascending LoS.

inated in this area during that phase. In particular the Albano polygenic crater was formed by at least 5 explosions occurred within a distance of  $\sim 1.5$  km and aligned along a NW-SE fracture system; the Ariccia and Nemi centres, formed by at least two coalescent craters, aligned along a general N-S direction [De Rita *et al.*, 1995]. The best constrained source is located beneath the Albano crater while the southern source is located  $\sim 3$  km south of the older Ariccia crater.

[15] The most recent and best located seismicity (1989–90 swarm) shows a general NW-SE trend and was characterised by hypocentral depths in the range 2–5 km beneath the Albano and Nemi lakes. As shown in Figure 1, south of the main swarm there is a subset of deeper (6–10 km) events also aligned in a general NW direction. Feuillet *et al.* [2004] explained the trend of the 1989–90 seismic swarm by modeling the total Coulomb stress resulting from the interaction of a spherical inflation source and a regional,  $N45^\circ$  extension.

[16] Our M2 model is in good agreement with both seismological and volcanological data.

[17] Ring faults and other structural discontinuities are known to play an important role in confining the surface deformation in caldera areas, with the net effect of reducing the depth resolution of elastic models [De Natale *et al.*, 1997]. No detailed information on location and geometry of structural features is available for the area, making impossible to quantify this effect, which would produce an increase of source depths. Therefore we consider the depths of the M2 sources (Table 1) as lower limits for realistic sources. Our simple elastic sources could be equally explained by pressurization of either a magma chamber or a hydrothermal reservoir.

## 6. Conclusion

[18] The Permanent Scatterers technique allowed the accurate measurement of the pattern of volcanic inflation in the Colli Albani area for the 1993–2000 period. By using ERS data from ascending and descending orbits, we could appreciate the E-W horizontal deformation, posing good constraints to the source depths. The modeled sources of deformation are in agreement with available geophysical

and volcanological data, and contribute to the comprehension of the present activity of the volcano.

[19] Unlike other Italian volcanoes, the Colli Albani has not undergone extensive monitoring for long time periods; this gap must be rapidly filled to lay the basis for a more complete assessment of volcanic hazard in such a strongly inhabited and vulnerable area.

[20] **Acknowledgments.** We thank A. Amato, E. D’Anastasio, L. Pizzino for fruitful discussions on different aspects of the research. Discussions with S. Cianetti and E. Trasatti and insightful comments from two anonymous referees, helped improve the modeling. The work was funded by INGV and ASI (contract 202-02). N. Feuillet has been supported by the EC Marie Curie Fellowship, contract HPMFC-CT-2000-01090.

## References

- Amato, A., and C. Chiarabba (1995), Recent uplift of the Alban Hills volcano (Italy): Evidence for a magmatic inflation?, *Geophys. Res. Lett.*, **22**, 1985–1988.
- Anzidei, M., P. Baldi, G. Casula, A. Galvani, F. Riguzzi, and A. Zanutta (1998), Evidence of active crustal deformation in the Colli Albani volcanic area (Central Italy) by GPS surveys, *J. Volcanol. Geotherm. Res.*, **80**, 55–65.
- Atzori, S. (2004), Algoritmi di inversione di dati geodetici SAR e GPS per la caratterizzazione geofisica di piani di faglia (in Italian), Ph.D. thesis, Univ. of Rome “La Sapienza,” Rome.
- Boni, C., P. Bono, S. Lombardi, L. Mastrolillo, and C. Percopo (1995), Hydrogeology, geochemistry and thermalism of the Alban Hills area, in *The Volcano of the Alban Hills*, edited by R. Trigila, pp. 221–242, Tipogr. SGS, Rome.
- Cayol, V., and F. H. Cornet (1998), Effects of topography on the interpretation of the deformation field of prominent volcanoes: Application to Etna, *Geophys. J. Int.*, **25**, 1979–1982.
- Chiarabba, C., A. Amato, and P. T. Delaney (1997), Crustal structure, evolution, and volcanic unrest of the Alban Hills, central Italy, *Bull. Volcanol.*, **59**, 161–170.
- De Natale, G., S. M. Petrazzuoli, and F. Pingue (1997), The effect of collapse structures on ground deformation in calderas, *Geophys. Res. Lett.*, **24**, 1555–1558.
- De Rita, D., R. Funicello, and C. Rosa (1992), Volcanic activity and drainage network evolution of the Alban Hills area (Rome, Italy), *Acta Volcanol.*, **2**, 185–198.
- De Rita, D., C. Faccenna, R. Funicello, and C. Rosa (1995), Stratigraphy and volcano tectonics, in *The Volcano of the Alban Hills*, edited by R. Trigila, pp. 33–71, Tipogr. SGS, Rome.
- Ferretti, A., C. Prati, and F. Rocca (2001), Permanent scatterers in SAR interferometry, *IEEE Trans. Geosci. Remote Sens.*, **39**(1), 8–20.
- Feuillet, N., C. Nostro, C. Chiarabba, and M. Cocco (2004), Coupling between earthquake swarms and volcanic unrest at the Alban Hills volcano (Italy) through elastic stress transfer, *J. Geophys. Res.*, **109**, B02308, doi:10.1029/2003JB002419.
- Funicello, R., G. Giordano, and D. De Rita (2003), The Albano maar lake (Colli Albani volcano, Italy): Recent volcanic activity and evidence of pre-Roman Age catastrophic lahar events, *J. Volcanol. Geotherm. Res.*, **123**, 43–61.
- Mogi, K. (1958), Relations between eruptions of various volcanoes and the deformation of the ground surface around them, *Bull. Earthquake Res. Inst. Univ. Tokyo*, **36**, 99–134.
- Okada, Y. (1985), Surface deformation due to shear and tensile faults in a half-space, *Bull. Seismol. Soc. Am.*, **75**, 1135–1154.
- Pizzino, L., G. Galli, C. Mancini, F. Quattrocchi, and P. Scarlato (2002), Natural gas hazard ( $CO_2$ ,  $^{222}Rn$ ) within a quiescent volcanic region and its relations with tectonics: The case of the Ciampino-Marino area, Alban Hills volcano, Italy, *Nat. Hazards*, **27**, 257–287.
- Sen, M., and P. L. Stoffa (1995), *Global Optimization Methods in Geophysical Inversion*, Elsevier Sci., New York.
- Yang, X. M., P. M. Davis, and J. H. Dieterich (1988), Deformation from inflation of a dipping finite prolate spheroid in an elastic half-space as a model for volcanic stressing, *J. Geophys. Res.*, **93**, 4249–4257.

J. Allievi, TeleRilevamento Europa, Milan, Italy.

S. Atzori, N. Feuillet, S. Salvi, S. Stramondo, and C. Tolomei, Istituto Nazionale di Geofisica e Vulcanologia, Via di Vigna Murata 605, I-00143 Roma, Italy. (salvi@ingv.it)

A. Ferretti, C. Prati, and F. Rocca, Dipartimento di Elettronica e Informazione, Politecnico di Milano, Milan, Italy.